Design and Motion Control of a Two-Wheel Inverted Pendulum Robot

Shiuh-Jer Huang, Su-Shean Chen, Sheam-Chyun Lin

Abstract—Two-wheel inverted pendulum robot (TWIPR) is designed with two-hub DC motors for human riding and motion control evaluation. In order to measure the tilt angle and angular velocity of the inverted pendulum robot, accelerometer and gyroscope sensors are chosen. The mobile robot's moving position and velocity were estimated based on DC motor built in hall sensors. The control kernel of this electric mobile robot is designed with embedded Arduino Nano microprocessor. A handle bar was designed to work as steering mechanism. The intelligent model-free fuzzy sliding mode control (FSMC) was employed as the main control algorithm for this mobile robot motion monitoring with different control purpose adjustment. The intelligent controllers were designed for balance control, and moving speed control purposes of this robot under different operation conditions and the control performance were evaluated based on experimental results.

Keywords—Balance control, speed control, intelligent controller and two wheel inverted pendulum.

I. INTRODUCTION

TWO-wheel mobile platform and humanoid mobile robot are interesting application of inverted pendulum system. Due to the mature control strategy and electronic technology, the two-wheel inverted vehicle system was designed as the short distance mobile tool. Grasser et al. [1] designed a JOE system and derived its dynamic model based on Newton's method. Pathak et al. [2] derived the dynamic model of TWIPR and employed model-based partial feedback linearization method to manipulate its moving speed and position. Chiu and Peng [3] proposed a two-control-loop scheme with inner loop for balancing control and outer loop for position control. Ren et al. [4] proposed a self-tuning PID controller for vehicle motion speed monitoring with velocity feedback signal to convert into inclining angle for balancing. Ding and Cheng [5] designed and evaluated their performances of double PID control and LQR control. Almeshal et al. [6] developed a double inverted pendulum robot with movable payload and moving on an inclined surface. Dai et al. [7] designed a 5-DOF TWIPR with additional movable weight and left-right lean degree, and designed two PID controllers for balancing control and vehicle moving speed control. Sinha et al. [8] derived the dynamics model of TWIPR and designed a controller for slope motion control based on sliding mode and Lyapunov theorems. The well-known TWIP vehicle is Segway designed by Dean

Kamen [9] with five gyroscope and two inclination sensors to derive vehicle information for motion control. General motor and Segway cooperated to design a two-person electric vehicle PUMA with 56 km/hr maximum speed and 56 km distance of travel for each electric charge [10].

Humans have been dreaming up to create intelligent robots for executing our commands to do mundane tasks and complete difficult or complex endeavors more than five hundred years [11]. Hirai [12] first proposed a practical wheeled robot having two arms and a video camera installed on the upper body for recognition purposes for intelligence judgment research. This shows that the humanoid robots will be the accompanying intelligent machines in our future life. In addition to the stable wheeled mobile robot, the inverted pendulum robot development is also an interesting research topics. Lee and Jung [13] and Jeong and Takahashi [14] developed an inverted pendulum robot and adopted gyro and tilting sensors for designing balancing and motion controller.

Since, all the world is ambitious to improve the atmosphere quality, the electric vehicle development is gained much attention in this decade. The TWIPR is suitable designed for the urban short distance transportation tool. The synchronization and velocity control problems for different urban road situations still need to be investigated. Here, a prototype TWIPR is built with two-hub motor, embedded gyroscope and accelerometer sensors. The model-free intelligent FSMC was designed to monitor the mobile robot balancing, moving speed control, and slope climbing control under different payload conditions.

II. SYSTEMS STRUCTURE OF TWIPR

The main frame of this TWIPR was made of 10 mm width aluminum plate to support one person's weight as shown in Fig. 1. It has a handle bar to adjust the moving speed and electronic differential. For the balancing and motion control purposes, 3-axe accelerometer sensor MMA7361 is chosen to measure the gravity direction for deriving inclination angle, 2-axe gyroscope LPY503AL was built to measure the angular velocity. The inclination angle estimated from accelerometer is

$$\theta \approx \frac{V_y - V_{basic} - \ddot{x}_{motor}}{V_z - V_{basic}} \qquad (1)$$

where V_{basic}, V_y and V_z are the accelerometer analog output voltage at 0 g, current y and z directions, respectively. $\ddot{x}_{motor}$ is the robot moving acceleration derived from two-hub motors angular position variation based on hall sensor feedback. The

Su-Shean Chen, Sheam-Chyun Lin are with the National Taiwan University of Science and Technology, Taipei, 106, Taiwan (e-mail: m10403401@mail.ntust.edu.tw, sclynn@mail.ntust.edu.tw).

Shiuh-Jer Huang is with the National Taiwan University of Science and Technology, Taipei, 106, Taiwan (corresponding author, phone: 886-2-27376449; fax: 886-2- 27376460, e-mail: sjhuang@mail.ntust.edu.tw).

mobile robot rotational velocity on x and z directions is measured by using embedded gyroscope.

$$\omega_x \approx 0.0017(V_x - V_{ref}) , \quad \omega_z \approx 0.0017(V_z - V_{ref}) \qquad (2)$$

where V_x, V_{ref} and V_z are the gyroscope analog output voltage measurement values.

In order to record the mobile robot motion information and update the MCU control program, Zbee S1 wireless communication module was selected to connect the MCU and PC with UART transmission interface. For simplifying the transmission structure of this mobile robot, 400-W three-phase permanent magnet DC brushless hub motor is chosen for each wheel. The tire outside diameter is 9.5 inch. Three built-in-hall sensors are used to derive the rotor angle for the robot's moving distance detecting and position control. The resolution is 300 counts per circle.

Since the ARduino Nano microprocessor has embedded flash memory to store control program and data, UART and I2C communication port, it was chosen as the control kernel of this TWIPR system. It also has two 8-bit timer counters equipped with PWM output and overflow interrupt and one 16-bit counter register. Here, timer2 overflow interrupt is set as fixed system control frequency 100 Hz. Timer1 generates 25 kHz high frequency PWM signal. This microprocessor also has

8-channel ADC for converting the sensors' analog feedback signals into digital for MCU control purpose. The wireless communication module was chosen to transfer the robot motion situation to outboard PC for analysis purpose without addition cable line. ATMEGA318 provides an 8-bit external interrupt port for pin change interrupt (PCINT) function. Here, the Port B and port D signals change interrupts are used to read in two-wheel hall sensor signals. The overall TWIPR system control board is shown in Fig. 2. A first order RC low pass filter is employed to suppress the noise of measured analog signal.
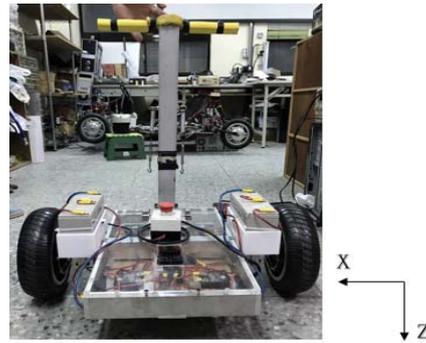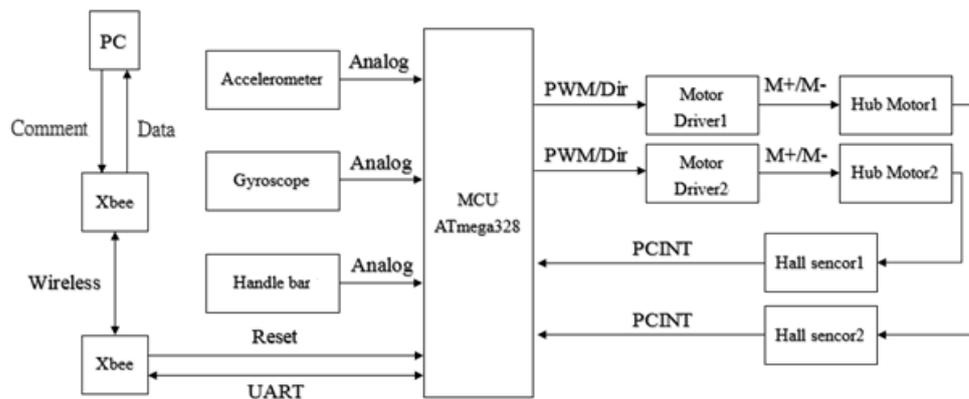

Fig. 1 TWIP vehicle side view

Fig. 2 TWIPR mechatronics system control block diagram

III. TWIPR DRIVING CONTROL

A. Motor Driver Circuit

The driver for three-phase DC blushless motor consists of a microprocessor (MCU), gate switch driver and up-low arm inverter circuit as shown in Fig. 3 (a). MCU extracted the signals from three motor-inside-hall sensors to obtain rotor position. The rotor $360°$ angle is divided into six $60°$ intervals. There are six different combinations of three phase current within a motor electrical cycle. MCU sends appropriate signal to change the gate driver on-off states in order to guarantee that the motor three-phase stator windings only have two windings with signals transmitted to inverter for driving motor. Each cycle has six-step square wave actuating to change electric

conduction states per $60°$ electric angle. Here, the motor driver circuit is a bridge type three-phase inverter with six MOSFET as shown in Fig. 3 (b). The MOSFET is TK80E08K3 of Toshiba com. with maximum 75 V and 80 A rated voltage and current, respectively. Triangular wave PWM scheme is chosen for monitoring control. The same PWM duty cycle was selected for MOSFET up arm switching with low arm normal open to implement square current wave tracking.

B. FSMC Control Algorithm

It is well known that inverted pendulum vehicle dynamic system has time-varying and complicate dynamics characteristics, the model based controller design is difficult to implement. Here, the model free intelligent FSMC scheme is planned as the key control strategy combining with certain

control scheme to design the balancing, and moving speed control laws for this TWIPR. The FSMC control strategy law

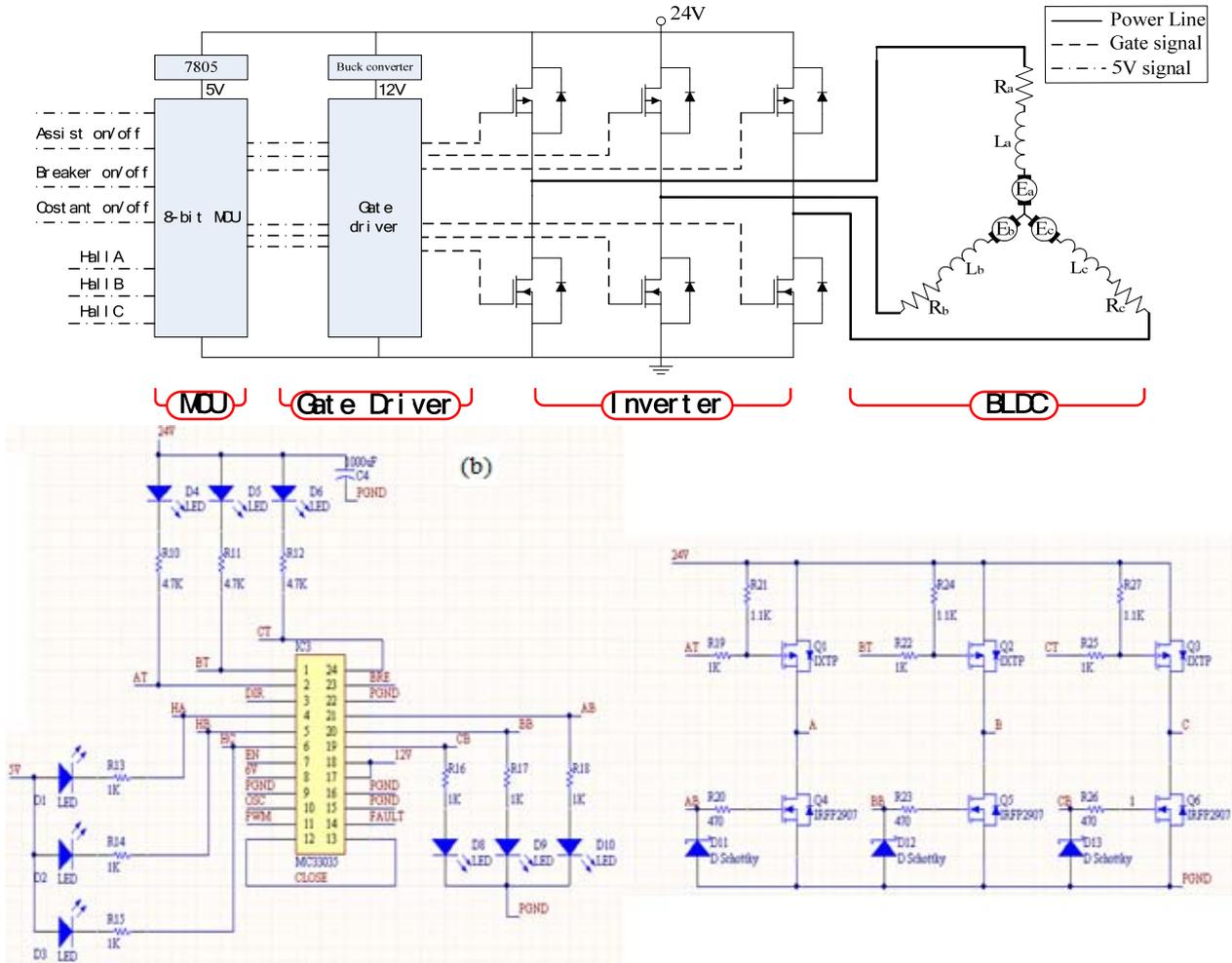brief explanation and each wheel control law are described in following sections.

Fig. 3 DC hub motor driver circuit: (a) structure and (b) circuit

A sliding surface on the phase plane is defined as

$$s(t) = (\frac{d}{dt} + \lambda)e_1 = e_2 + \lambda e_1 \qquad (3)$$

where $e_i = \theta_{id} - \theta_i$ are defined as the wheel angular state control errors. A fuzzy logic control system is designed based on the sliding variable, s, to approximate the specified perfect control law, u_{eq} of sliding mode control. If this perfect control law is derivable, the asymptotical stability dynamic behavior can be achieved for this closed loop control system as.

$$\dot{s}(t) + \lambda s(t) = 0 \qquad (4)$$

where λ is a positive design parameter. Hence, the sliding surface variable, s, will gradually converge to zero. Since, the sliding surface variable, s, is defined as error states

combination as (4), the system output error will converge to zero theoretically, too. Here, the fuzzy approximated perfect control law for each sampling step control voltage change is derived from fuzzy inference and defuzzification calculation instead of the equivalent control law derived from the nominal system dynamics model at the sliding surface. This control structure has two advantages. The first one is that it can eliminate the chattering phenomenon of a traditional sliding mode control. The second one is that the mathematical model and constant gain limitation are not required in controller design process. Fig. 4 demonstrates this system control block diagram. The sliding surface reaching condition, $s \cdot \dot{s} < 0$ is employed to design the simplified one-dimensional fuzzy rules based on the sliding surface input variable, s. In general, the fuzzy input/output variables are fuzzilized with different number of fuzzy sets within the universe of discourse of -1 and +1. Here, equal span 11 fuzzy membership functions subsets within the range of -1 and +1 were chosen to fuzzy the input

and output variables. Hence, a scaling factor gs for the sliding surface variable, s, and a scaling factor gu for the control

voltage are designed to map the variables into this universe of discourse and adjust the control voltage value, respectively.
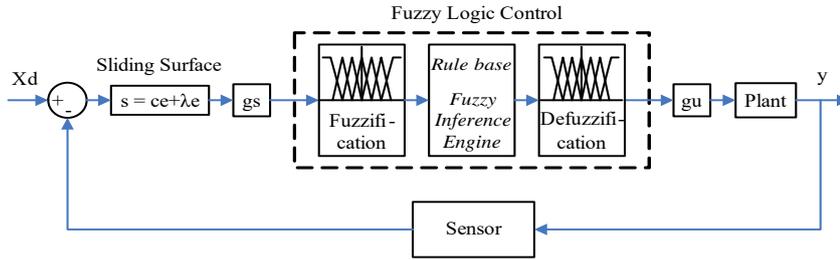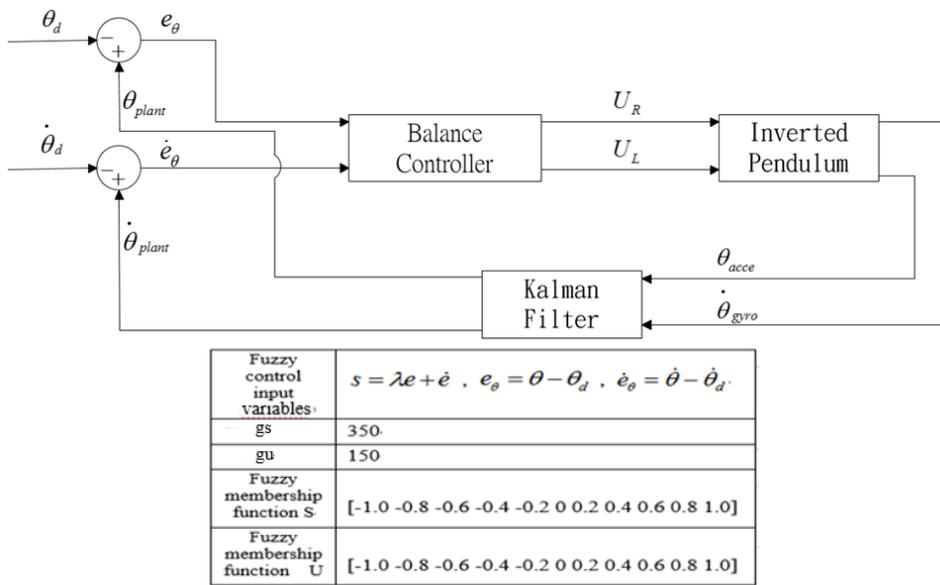

Fig. 4 FSMC block diagram

Fuzzy control input variables	$s = \lambda e + \dot{e}$, $e_\theta = \theta - \theta_d$, $\dot{e}_\theta = \dot{\theta} - \dot{\theta}_d$.
gs	350
gu	150
Fuzzy membership function S	[-1.0 -0.8 -0.6 -0.4 -0.2 0 0.2 0.4 0.6 0.8 1.0]
Fuzzy membership function U	[-1.0 -0.8 -0.6 -0.4 -0.2 0 0.2 0.4 0.6 0.8 1.0]

Fig. 5 System control block diagram and control parameters of balancing controller

C. Mobile TWIPR Balancing Control

Since the TWIPR system is an unstable dynamic system, the most basic requirement of its operation is to design the balancing control strategy. In this study, the balancing controller is designed based on the previous described FSMC control scheme. Due to the dynamics balancing concept, if the mobile robot posture is forward leaned, the robot should move forward for eliminating the forward momentum and maintaining stable up-right position. Conversely, mobile robot should move backward to overcome robot leaning back momentum. Hence, the inclination angular error and angular speed error were chosen as input signals for the FSMC balance controller to derive the PWM duty cycle for the wheel motors control input. The system control block diagram and control parameters of this balancing controller are shown in Fig. 5.

D. The Mobile Robot Moving Speed Control

Actually, two wheel motors with the same speed command may have obviously wheel speed difference due to mechanism and electric components variation. That will induce mobile

robot motion path deviation, especially obvious in long distance travelling. In this experimental system, two wheel motors of this TWIPR were manipulated with their individual controller and driving circuit. Hence, a synchronous controller for both wheel motors should be designed firstly to compensate this phenomenon for further robot motion path or parking position control. Here, a FSMC controller is designed based on two-wheel position error e_{p-diff} and velocity error $\dot{e}_{p-diff}$ inputs to obtain the PWM duty cycle compensation value for the left hub motor control input adjustment. This compensation function is represented as a "two-wheel synchronous controller control block" in motion speed system control block diagram in Fig. 6. The variables P_{w-d} and V_{w-d} are two-wheel electric differential commands for turning purpose. They should be set as zero for two-wheel synchronous control without speed difference.

Based on robot balancing control strategy, the leaning forward vehicle posture ($\theta > 0^{\circ}$) will generate motor positive rotation to bring the robot moving forward. The handle bar will

induce forward torque on robot body and cause inclination angle increased gradually during robot moving forward. Then, the robot moving speed will increase gradually till it loses stable balancing. Hence, a speed controller should be designed to adjust the robot mass central position for achieving the stable constant moving speed function. Here, the FSMC controller is

designed with vehicle speed error $e_v = V - V_d$ and acceleration error $\dot{e}_v = \dot{V} - \dot{V}_d$ as input signals to obtain the robot posture inclination angle command value $\theta_{command}$. The system control block diagram and the control parameters are listed in Fig. 6.
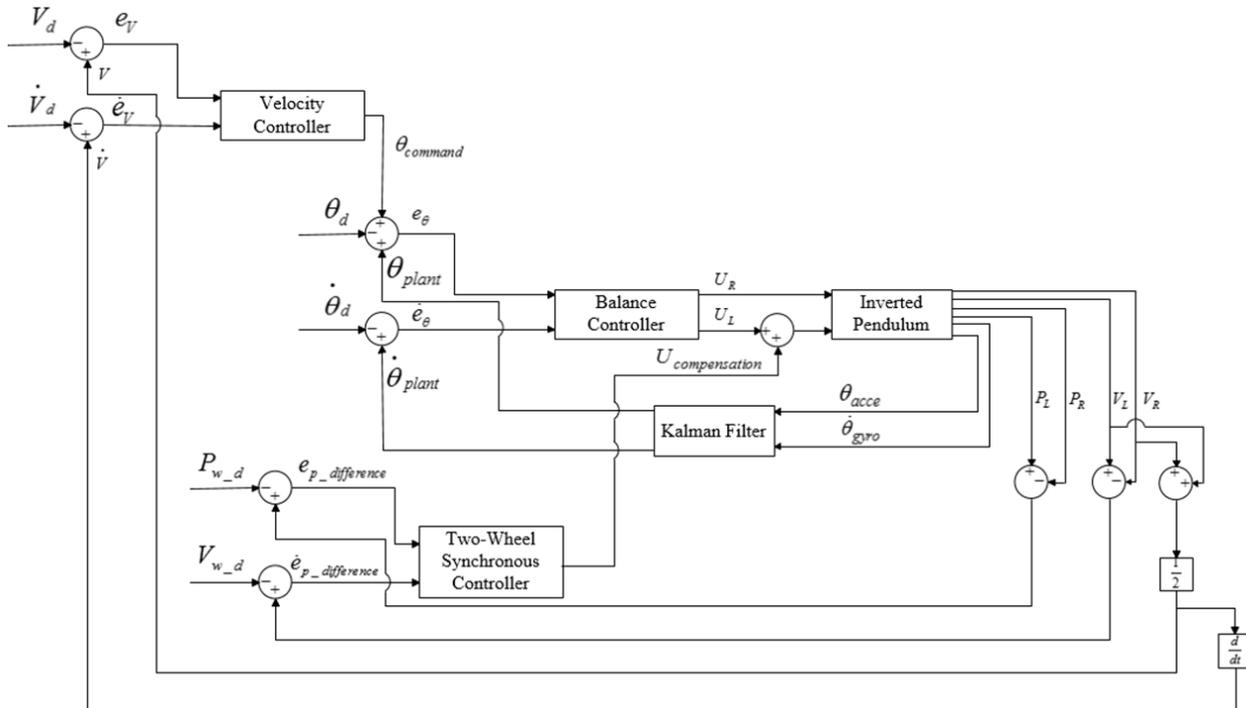
fuzzy control input variables	$s = \lambda e + \dot{e}$, , $e_{p\_difference} = (P_L - P_R) - P_{w\_d}$ $\dot{e}_{p\_difference} = (\dot{P}_L - \dot{P}_R) - \dot{P}_{w\_d}$, $e_v = V - V_d$
gs	60
gu	50
fuzzy membership function S	[-1.0 -0.8 -0.6 -0.4 -0.2 0 0.2 0.4 0.6 0.8 1.0]
fuzzy membership function U	[-1.0 -0.85 -0.6 -0.4 -0.2 0 0.2 0.4 0.6 0.85 1.0]

Fig. 6 Mobile robot control block diagram and control parameters

IV. EXPERIMENTAL RESULTS

Here, the model free intelligent FSMC scheme is employed as the kernel control strategy to design the balancing, and moving speed control laws for this TWIPR system. The mobile robot closed loop sampling frequency is set as 100 Hz for following experiments. The robot motion dynamics information was derived from the two-wheel motion speeds and rotation angles. They were transmitted to PC through XBee wireless communication module with 20 Hz frequency for further dynamic response and data analysis purpose. The PC record data include mobile robot inclination angular velocity (mrad/sec) of gyroscope, robot inclination angle (mrad), motor hall sensor and change rate and motor PWM control signal. Those signal were converted into robot inclination angle

(degree), angular velocity (degree/s), moving distance (m) and velocity (m/sec), and hob motor control voltage (V) by MATLAB tool box for figure plotting and analysis.

A. Mobile Robot Balancing Control

Single control law value is derived from FSMC controller to monitor both hub motor back and forth motion, simultaneously. The FSMC control rules were listed in Fig. 5. The experimental results of TWIPR tilt angle, control voltage and tilt angle phase diagram response during 30 seconds balancing control are shown in Figs. 7 (a)-(c), respectively. In the beginning, the robot has a negative tilt angle, the mobile robot is in a backward situation. The balancing controller is actuated to regulate the robot back and forth motion for maintaining stable up-right

situation. The experimental results show that the robot tilt angle is controlled within in 0.2°. The RMS of vehicle tile angle during 30 seconds control period is 0.065° of this study. The robot tilting phase diagram has a very good stable response.
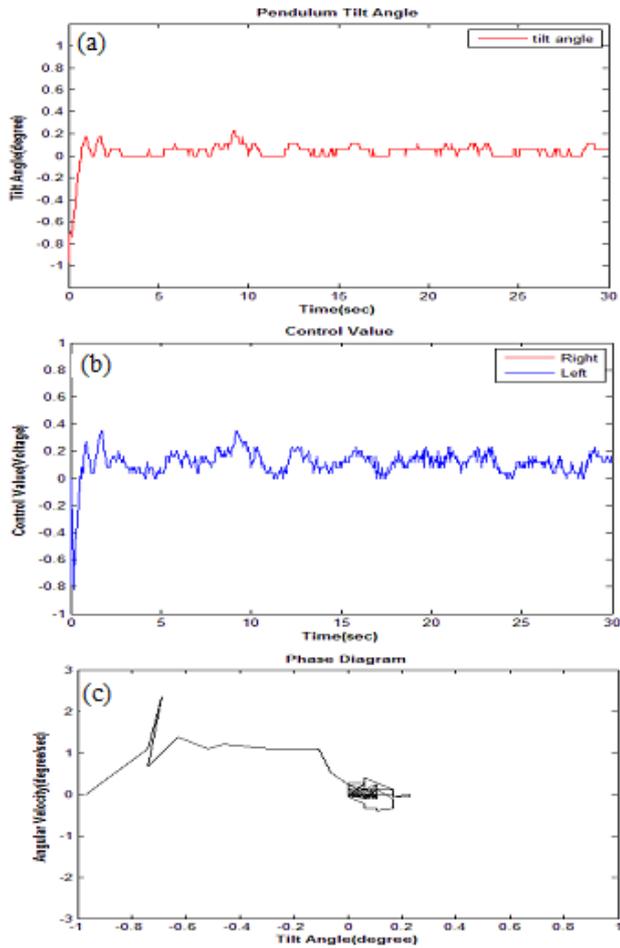

Fig. 7 (a) Robot tilt angle, (b) control voltage and (c) tilt angle phase diagram responses during 30 seconds balancing control

B. Robot Moving Speed Control With/Without Human Payload

The FSMC control parameters and fuzzy control rules are listed in Fig. 6. Here, the control purpose is to monitor the mobile robot 0.2 m/s travelling speed within 15 seconds. In the first 5 seconds, the robot is maintaining balancing. During 5 to 14 seconds, the robot is commanded to move with 0.2 m/s speed and 14-15 seconds the robot is commanded to stop. The experimental results of TWIPR tilt angle, both wheels travelling velocity and positions response during 15 seconds balancing control are shown in Figs. 8 (a)-(c), respectively. The mobile robot setting speed is reached within 2 seconds and with the speed error oscillation amplitude less than 0.02 m/s. The robot tile angle has a smooth response during this speed control process. When the mobile robot has a human with 70-kg weight onboard, the experimental results of TWIPR tilt angle,

both wheels travelling velocity and positions response during 30 seconds balancing control are shown in Figs. 9 (a)-(c), respectively. Since the onboard human has the self-balancing tendency, that will interfere the controller operation. However, the mobile robot still can maintain the stable constant speed command operation with tile angle variation less than 2.5° and the speed oscillation amplitude less than 0.03 m/s.
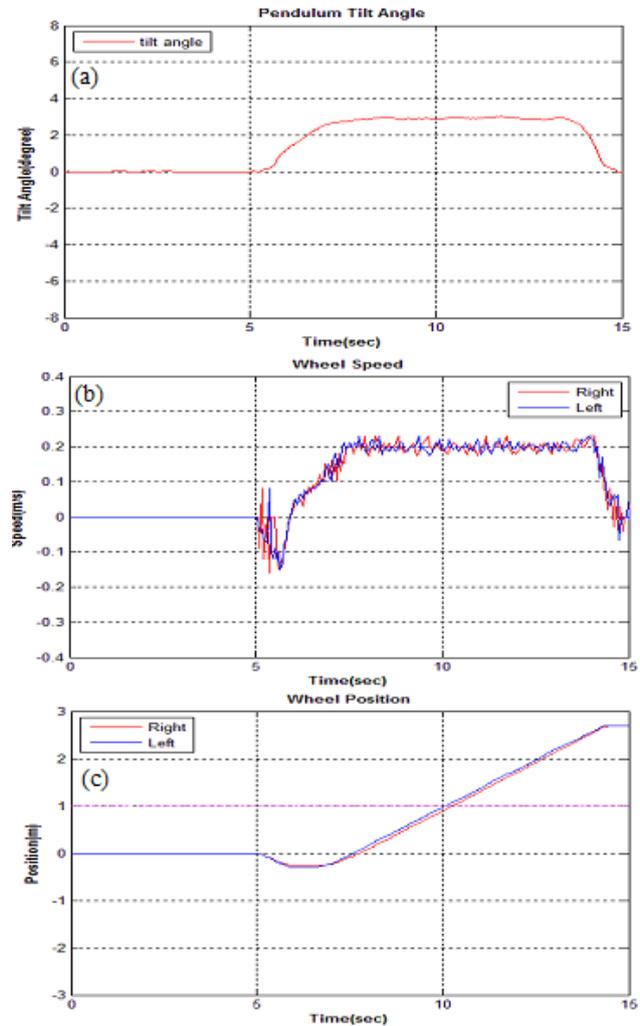

Fig. 8 (a) Robot tilt angle, (b) both wheels travelling velocity, and (c) positions responses during 15 seconds speed control

C. Robot Move up a Slope with 0.2 m/s Constant Speed

The mobile robot is commanded to move up a 30°pavement slope with 0.2 m/s constant speed. In the first 5 seconds, the robot is maintaining balancing. During 5 to 14 seconds, the robot is commanded to move up slope with 0.2 m/s speed and 14-15 seconds, the robot is commanded to stop. The experimental results of TWIPR tilt angle, both wheels control voltages, travelling velocity and positions response during 15 seconds balancing control are shown in Figs. 10 (a)-(d), respectively. At the beginning instant (5th sec.), the control law provides a negative control voltage for the wheel to achieve the

setting tilting angle. Then, the wheel moves back and the robot body lean forward for robot to climb up. Since, the slope surface is not smoothness, and the robot motion dynamics and central gravity has significant variation, the tilt angle and both wheels moving speed have significant variation. However, the mobile robot still can maintain the stable constant speed command operation with tile angle variation less than 5° and the speed oscillation amplitude less than 0.035 m/s.

V. CONCLUSION

A TWIPR mobile robot system was constructed with embedded system control structure for short distance motion control evaluation. The intelligent FSMC control strategy was proposed to design the balancing, two-wheel synchronous motion, and robot moving speed control, respectively. The mobile robot velocity control error is less than 3 cm/s for with/without human payload and slope climbing up operation conditions. This means that the proposed control structure is a general purpose solution for TWIPR applications.
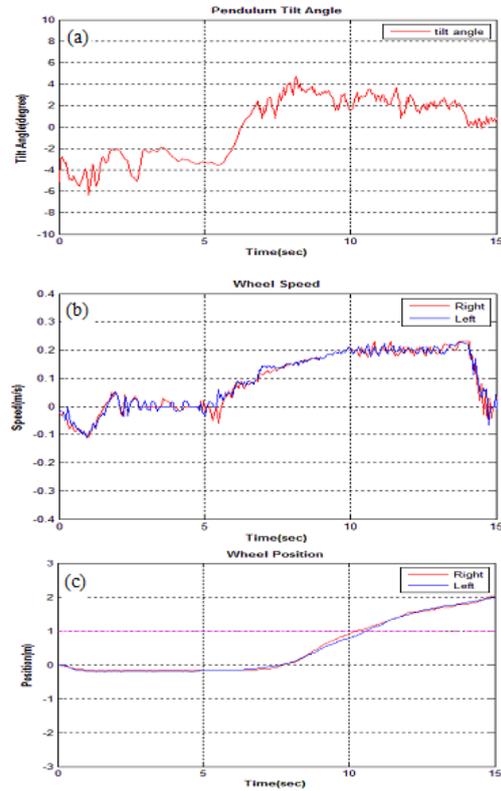

Fig. 9 (a) Robot tilt angle, (b) both wheels travelling velocity, and (c) positions responses during 15 seconds speed control with human payload
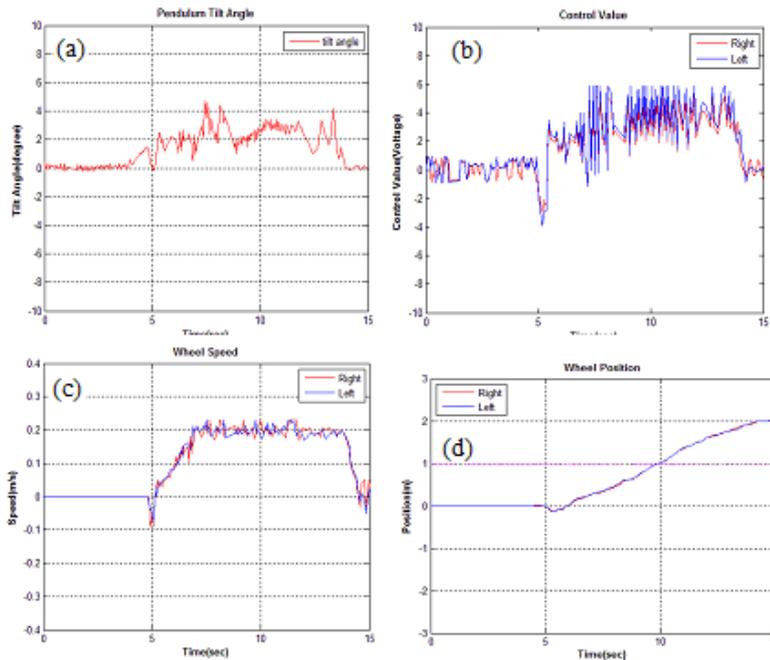

Fig. 10 (a) Robot tilt angle, (b) both wheels control voltages, (c) both wheels travelling velocity, and (d) positions responses during 15 seconds climbing slope speed control

REFERENCES

[1] F. Grasser, A. D'Arrigo, S. Colombi, A. C. Rufer, "JOE: a mobile, inverted pendulum," IEEE Transactions on Industrial Electronics, Vol. 49, 2002.

[2] K. Pathak, J. Franch, S.K. Agrawal, "Velocity and position control of a wheeled inverted pendulum by partial feedback linearization," IEEE Transactions on Robotics, Vol. 21, 2005.

[3] C. H. Chiu, and Y. F. Peng, "Design and Implementation of the self-dynamic Controller for Two-Wheel Transporter," IEEE International Conference on Fuzzy Systems, 2006.

[4] T. J. Ren, T. C. Chen, and C. J. Chen, "Motion control for a two-wheeled vehicle using a self-tuning PID controller." Control Engineering Practice, pp. 365-375, 2007.

[5] W. Li, H, Ding, and K, Cheng, "An Investigation on the Design and Performance Assessment of double-PID and LQR Controllers for the Inverted pendulum," UKACC International Conference on Control, Cardiff, United Kingdom, pp.190-196, September 2012.

[6] A. M. Almeshal, K. M. Goher, and M. O. Tokhi, "A new configuration of a two-wheeled double inverted pendulum-like robotic vehicle with movable payload on an inclined plane, " First International Conference on Innovative Engineering Systems (ICIES),Dec 2012.

[7] Fuquan Dai, Jize Li, Jinmin Peng, "Design and control of multi-DOF two wheeled inverted pendulum robot," 11th World Congress on Intelligent Control and Automation (WCICA), July 2014.

[8] Abhinav Sinha, Pikesh Prasoon, Prashant Kumar Bharadwaj, "Nonlinear autonomous control of a two-wheeled inverted pendulum mobile robot based on sliding mode," International Conference on Computational Intelligence and Networks (CINE), Jan 2015.

[9] Segway of West Texas, "i2 Models," Retrieved July 1, 2015, from http://www.segwaytexaswest.com/i2%20Models.htm.

[10] Segway's P.U.M.A., Retrieved July 7, 2017, from http://www.segway.com/puma/.

[11] P. Sareh and M. Kovac, "Mechanized creatures," Science, Vol. 355, No. 6332, pp. 1379.

[12] K. Hirai, "Current and future perspective of Honda humanoid robot," Proc. Of the 1997 IEEE/RSJ International Conference on Intelligent Robots and Systems, 1997.

[13] H. J. Lee and Seul Jung, "Control of a mobile inverted pendulum robot system," International Conference on Control, Automation and Systems, 2008.

[14] S. H. Jeong and Takayuki Takahashi, "Wheeled inverted pendulum type assistant robot: Inverted mobile and Sitting motion," IEEE/RSJ International Conference on Intelligent Robots and Systems, pp. 1932-1937, 2007.

Shiuh-Jer Huang received the B.Sc. and M.Sc. degrees form National Taiwan University, Taipei, TAIWAN, in 1978, 1980, and the Ph.D. degree from the University of California, Los Angeles, in 1986, all in mechanical engineering department. In 1986, he joined the faculty of the Department of Mechanical Engineering, National Taiwan University of Science and Technology, Taipei, TAIWAN, where he is currently a professor. His research interests are robotic system control and applications, vibration control, Mechatronics, and vehicle active suspension control.

Su-Shean Chen is a graduate student in Department of Mechanical Engineering, National Taiwan University of Science and Technology, Taipei, Taiwan.

Sheam-Chyun Lin received the Ph. D degree from Oklahoma University in 1987, in mechanical engineering department. Then, he joined the faculty of the Department of Mechanical Engineering, National Taiwan University of Science and Technology, Taipei, TAIWAN, where he is currently a professor. His research interests are fluid mechanics and cooling fan design and analysis.